Tactile and Chemical Sensing With Haptic Feedback for a Telepresence Explosive Ordnance Disposal Robot

Chenxi Xiao, *Member, IEEE*, Aaron Benjamin Woeppel, Gina Marie Clepper, *Member, IEEE*, Shengjie Gao, Shujia Xu, Johannes F. Rueschen, Daniel Kruse, Wenzhuo Wu, *Senior Member, IEEE*, Hong Z. Tan, *Fellow, IEEE*, Thomas Low, Stephen P. Beaudoin, Bryan W. Boudouris, William G. Haris, and Juan P. Wachs, *Senior Member, IEEE*

***Abstract*—Robots can be used to mitigate risks in unsafe and austere settings. In recent years, explosive ordnance disposal robots have reduced the technician's time-on-target, and thus, reduce the direct risk of exposure. This article focuses on the study and development of innovative techniques as the foundational work for a new robot platform. The proposed system includes an organic electrochemical transistor device to detect the existence of explosive residues, and lead to decisions for safe-removal progress. Taurus' surgical gripper facilitates object tactile exploration, and manipulation with control precision to the millimeter range. The highly sensitive triboelectric tactile sensor could reduce intrusiveness during contact, and mitigate the risk of detonation. Haptic devices and visual displays are used to convey important signals, in order to improve the situational awareness of the teleoperator. A machine learning classifier can be used to assist the user to identify objects from tactile sampling. The integration of these methodologies allows for a sensitive approach to concealed objects that are only accessible through tactile sensing.**

Manuscript received 3 August 2022; revised 11 February 2023; accepted 12 April 2023. This material was supported in part by the National Science Foundation under Grant NSF NRI #1925194 and Grant NSF #2140612. This paper was recommended for publication by Associate Editor S. F. Atashzar and Editor E. Yoshida upon evaluation of the reviewers' comments. *(Corresponding author: Juan P. Wachs.)*

This work involved human subjects or animals in its research. Approval of all ethical and experimental procedures and protocols was granted by Purdue University Institute Review Board (IRB) under Application No. 611004681, and performed in line with the Declaration of Helsinki.

Chenxi Xiao, Shengjie Gao, Shujia Xu, Wenzhuo Wu, and Juan P. Wachs are with the School of Industrial Engineering, Purdue University, West Lafayette, IN 47907 USA (e-mail: xiao237@purdue.edu; gao401@purdue.edu; xu1377@purdue.edu; wu966@purdue.edu; jpwachs@purdue.edu).

Aaron Benjamin Woeppel, Stephen P. Beaudoin, and Bryan W. Boudouris are with the Davidson School of Chemical Engineering, Purdue University, West Lafayette, IN 47907 USA (e-mail: awoeppel@purdue.edu; sbeaudoi@purdue.edu; boudouris@purdue.edu).

Gina Marie Clepper, Johannes F. Rueschen, and Hong Z. Tan are with the Elmore Family School of Electrical and Computer Engineering, Purdue University, West Lafayette, IN 47907 USA (e-mail: gclepper@purdue.edu; jruesche@purdue.edu; hongtan@purdue.edu).

Daniel Kruse and Thomas Low are with the SRI International, Menlo Park, CA 94025 USA (e-mail: krused2@rpi.edu; thomas.low@sri.com).

William G. Haris is with the United States Navy, Naval Surface Warfare Center Indian Head Division (NSWC IHD), Indian Head, MD 20640 USA (e-mail: william.g.haris.civ@us.navy.mil).

This article has supplementary material provided by the authors and color versions of one or more figures available at https://doi.org/10.1109/TRO.2023.3278455.

Digital Object Identifier 10.1109/TRO.2023.3278455

***Index Terms*—Haptics and haptic interfaces, nanomanufacturing, robotics in hazardous fields, soft sensors and actuators.**

I. Introduction

EXPLOSIVE ordnance disposal (EOD) is known to be among the most hazardous occupations [1]. When confronted with improvised explosive devices (IEDs), most EOD operations target to dispose of the exposed explosive materials expeditiously and safely while minimizing collateral damage. The EOD technicians are trained to recognize, identify, and often analyze the explosive materials, in order to disarm and render them safe for disposal. In hazardous environments, protective suits, helmets, and heavy steel blast shields provide the necessary protection again blast injuries [2]. While the impact from blasts can be mitigated, the protection may not be completely effective against direct exposures, leading to physical injuries [3]. Additionally, the protective equipment is heavy and constrains movement, introducing fatigue, heat stress, and reduced dexterity in onsite operations [4].

To mitigate these problems in hazardous environments, EOD robots have been deployed to disposal tasks, reducing the risks in otherwise deadly scenarios. Most EOD robots are based on some form of teleoperation, in which the technicians need to play the role of teleoperators who control the robot from afar [5], [6]. The remote control is established by a bidirectional communication link that transfers the control command and observation feedback between human and robotics in real time. On the negative side, the use of telerobots limits situational awareness [7], especially considering that current available EOD robots build heavily on the visual telemetry [8]. Such low situational awareness can impair the ability to detect IEDs that are not exposed, such as those that are concealed or buried [9]. Within controlled environments, ordnance disassembly attempts to remove energetics for ordnance preservation. Some operations require increased risk exposure for the technician to validate inert status.

This article proposes a suite of algorithms and techniques that can improve situational awareness in such teleoperation tasks by multimodality sensory feedback. The multimodal information consists of vision, tactile, and the chemical composition of the

target object. The resulting multimodal signals are used by the teleoperator to enhance decision making regarding risk level, proper disposal, and manipulation strategies of the explosive residues in question. Likewise, the usage of tactile feedback will allow operators to feel the object with their arms and hands through haptics. This allows them to understand object shape, structure, and composition [10]. Tactile feedback is also designed to assure safe interaction with objects in an unintrusive fashion [11]. This is critical as minimal changes can lead to inadvertent detonation.

From the human side, this work also aims to improve situational awareness through tactile display methods based on visual and haptic channels. Using the accumulated observations, object shape can be recovered based on accumulated contact signatures that are intrinsically sparse and discrete [12]. The semantic information that requires immediate attention is conveyed through a pair of haptic sleeves that exploits the information bandwidth of the human skin [13]. The information is transmitted using vibrotactile patterns that are optimized for the human perceptual system [14].

The current manuscript presents a consolidated robotic system where several modules can be integrated, and combined to achieve the purpose of bomb dismantling with the "human in the loop." Some of these modules appeared individually in published conference papers [14], [15] or journal papers [12], as stand-alone papers. However, the emphasis of this article has the merit on the innovation in integration of the different modules. Therefore, for completeness purposes, we discuss different components in the context of the complete system, providing citations and references to the aforementioned published works without repeating material that has been published. For the comprehensiveness of the system, the contents in [12] are briefly summarized. However, this article did not evolve from it. In addition, there are other novel aspects in this article, such as the novel organic electrochemical transistor (OECT)-based chemical sensor that can characterize explosive residues, which were not presented in previous articles.

The rest of this article is organized as follows. A literature review of the technologies relevant to our EOD robot, tactile sensing, and haptic rendering is given in Section II. The robot platform and the overall system architecture are introduced in Section III. Design principles of the OECT device for detecting explosive residues are given in Section IV. The mechanism and the fabrication process of the triboelectric nanogenerator (TENG) tactile sensor in are provided in Section V. Algorithms for visualization and object recognition based on tactile samples are given in Section VI. Methodology for rendering multimodal sensor signals is given in Section VII. Experiment results are provided in Section VIII; discussions are given in Section IX. Finally, Section X concludes this article.

In relation to the existing literature, our contributions include the following.

1) A tactile-based teleoperation framework that can operate effectively in scenarios where visual information is ineffective or unavailable.
2) An OECT device that enables the detection of explosive residues.
3) Integration of tactile sensors and haptic display devices for safe interaction with hazardous objects.
4) Haptic and visual rendering methods that provide assistance for EOD robot teleoperation.

II. Related Work

A. Explosive Detection

Safe detection, identification, and proper rendering safe of explosives has been a concern as urbanization extends to regions that have been used as "hot zones" between groups in armed conflicts, as often these buffer zones were delimited by mines [16]. Since then, there has been a growing interest in technologies that allow explosive detection and safe rendering while minimizing the time on target and direct exposure of technicians to threats. A common practice for explosive disposal is either direct remote detonation, or defeat and disposal in cases where detonation is not feasible or can have devastating effects. When there is a question about the composition of the threat, explosive detection is conducted first. Explosive detection can either employ bulk detection or, as applicable to this work, trace detection (ETD) [17], focused on examining residue on the surface of the the package of interest. ETD includes various means which encompasses techniques such as mass spectrometry/ion mobility spectrometry [18], animal olfactory detection [19], and electronic noses [20]. To et al. [21] provided a recent and extensive discussion of various mechanisms of ETD. Previous efforts were shown by Caygill et al. [22], where a sensor or electronic nose ETD detection scheme was proposed. Such EOD sensors can easily be installed on the robot and swabbing residue can be quickly accomplished via remote operation. An extensive amount of work in ETD sensors was allocated for the detection of commercial explosives, such as nitroaromatics [23]. Those solutions are not suitable for improvised explosives, especially ammonium nitrate mixtures, which are becoming exceedingly common [24], [25]. Hence, there is need to continue to work toward new sensing technologies that can effectively detect both commercial and improvised explosives, and at the same time, dispose the explosive from afar.

To this end, sensor information is passed to an offsite operator as a quantitative result (e.g., a change in mass or current). To do so, two potential schemes for the development of these sensors are: electrochemical [26], [27] and chemiresistive sensors. These sensors measure currents resulting either from a transfer of electrons between the sensor and analyte or as a result of absorption of an analyte into an active material. Importantly, while electrochemical sensors can detect explosives in vapor or solution phase [28], [29], chemiresistive sensors are limited to vapor phase detection—a concern for detecting nonvolatile or hermetically sealed materials. However, both schemes' working principles can be incorporated into a solution phase sensor by using an OECT.

An OECT uses a similar geometry and operation principle to a metal–oxide–semiconductor field effect transistor (see Fig. 1) however, it contains a semiconducting polymer channel (rather than an inorganic semiconductor) whose resistance is tuned

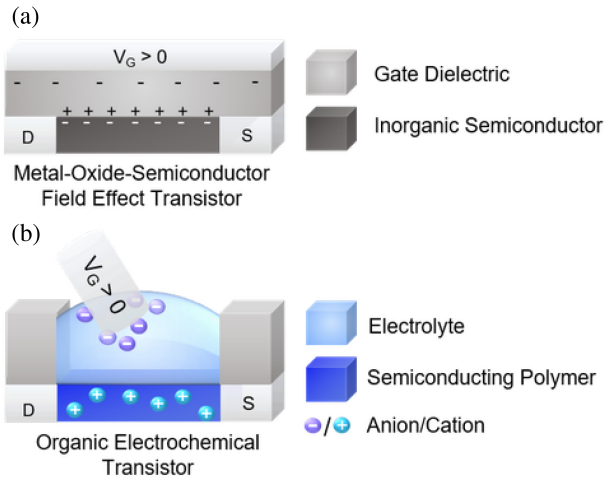

Fig. 1. Comparison of the device structure of (a) metal–oxide–semiconductor field effect transistor and (b) organic electrochemical transistor (OECT).

via an adjacent electrolyte gate (rather than a solid insulating dielectric) [30]. During typical operation, the gate bias produces an electric field, which drives dissolved ions from the electrolyte into the semiconducting polymer channel, introducing or compensating excess charge carriers [31], [32]. OECTs are flexible, compact, and use biocompatible materials; these attractive properties make them particularly strong candidates for bioelectronics [33] and biosensing. Here, their flexibility and small size is suitable for ETD applications. OECT's application for biosensing stems from their ease of modification [34], [35]—at gate and channel interfaces [36], [37], [38]. Their potential viability for remote ETD stems from their solution phase sensing mechanism—bypassing the concern of low explosive vapor pressure [39], and they are low-power demand, and micron scale in size allowing for ease of installation. In this work, we will use a simple OECT design to demonstrate how basic OECT operation can be applied to identify ammonium nitrate collected from residue.

B. EOD Robots

Robots have been deployed to EOD tasks to eliminate the risk of an otherwise deadly scenario. For example, the TALON robot is a telerobot with mounted cameras and a dexterous manipulator, which enables it to view, grip, cut, and move IEDs [40]. IRobot PackBot EOD robot platform is a portable mobile platform equipped with a seven degree-of-freedom (DOF) manipulator, which allows a specialist to remotely disarm IEDs [41]. Other similar robot platforms include tEODor [42], the Vanguard MK2 (Allen-Vanguard), Hornet MK-5 (InRob Tech Ltd), the Wheelbarrow series (British Army), SILO-6 [43], and the SOLEM system (Foster Miller), among others.

The mobility of EOD robots is provided by a moving vehicle based on wheels or tracks. When detonation is needed, disruptors can be installed. In other cases, a manipulator arm is one of the most frequently used tool [44]. Many EOD robots are also capable of carrying multiple sensors and tools. For typical designs, the Wheelbarrow EOD robot can be equipped with cameras, weapons, and chemical detection devices. The SOLEM system was featured with night vision and thermal imaging to enhance the visual perception. Other sensors for distance measurements [45], or detecting chemical, biological, radiological, and nuclear threats can also be equipped by EOD robots based on the need of the task, as reported in literature [46].

EOD robots are usually controlled through computer interfaces, where EOD technicians are part of the loop [8], [41], [42]. In particular, reducing the interaction force when dealing with IEDs is a concern because it would otherwise lead to detonation without proper mitigation strategies. Haptic feedback can enable teleoperators to feel the interaction force at their own hands, which allows accurate dexterity and force, regulating the contact at a fine scale. Nevertheless, such tactile feedback has not yet been widely used [8]. There have been studies exploring the use of haptic feedback for EOD robots. Kang et al. [47] designed the haptic device for ROBHAZ-DT2 robot, which can convey the measured force and torque to the teleoperator. A force-based bimanual haptic telepresence system for demining was developed in [9], allowing better characterization of mines buried underground. Nahavandi et al. [48] present the HE-CIED robot, which can convey the gripping force to the teleoperator through a haptically -enabled gripper controller. Wormley et al. [49] present Robo Sally, a bimanual robot control system with bionic robot hands that could incorporate haptic feedbacks.

C. Triboelectric Tactile Sensor

Tactile sensors enable safe object engagement during teleoperation [50]. The availability of force or pressure information enables awareness of the active force, hence reducing the intrusiveness associated with object manipulation. This is critical for EOD disposal operations, as even slight stresses can result in detonation. Tactile sensors have already been included into manipulators, footpads, and artificial skins in robots. This article will focus on triboelectric tactile devices for the following reasons. First, the triboelectric tactile sensor may help in the material or explosive classification by providing feedback via one or more modalities. This is especially advantageous when studying objects that are not visible. The triboelectric effect is also known to be capable of characterizing material information quickly and accurately [51]. Second, the triboelectric sensor only needs a single electrode per taxel to be connected to a circuit [52], allowing flexible designs for space-sensitive applications such as remote bomb disposal and telesurgery.

D. Tactile Display

Tactile displays can be used to present pertinent information to a telerobotic operator, offloading some information from the audio and visual domains. A large body of research exists on the use of haptic feedback for navigation and object exploration, particularly in situations where visual feedback is not available. Tappeiner et al. [53] studied the impact of haptic feedback for discovery of buried objects in loose sand using bimanual teleoperation. The authors found that augmenting the visual feedback with a novel Touch and Guide in Tandem haptic feedback method led to enhanced performance, reduced

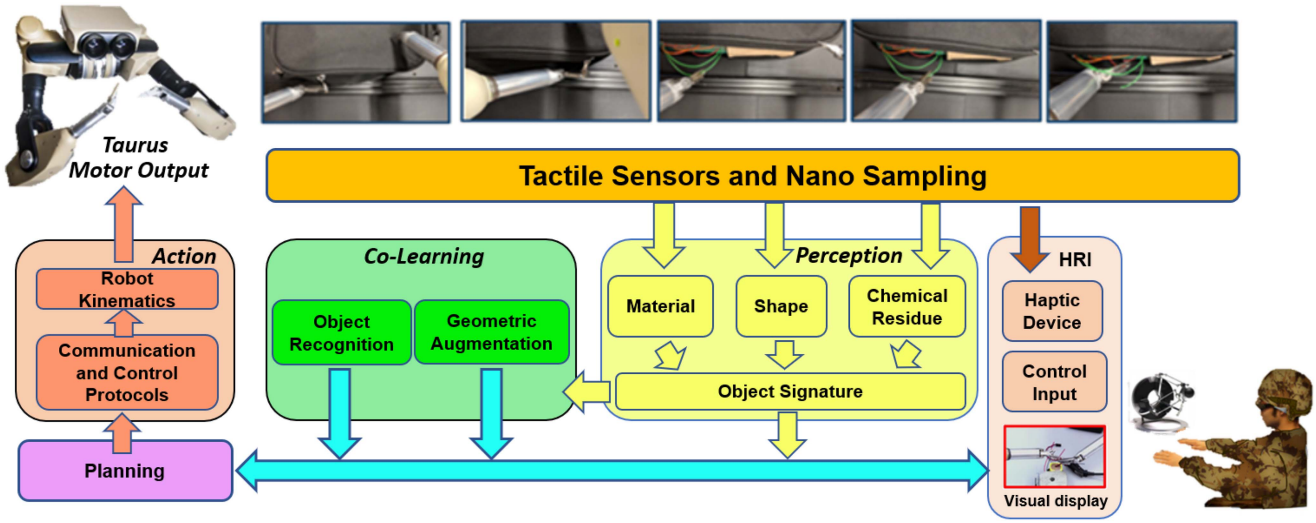

Fig. 2. Robot platform we developed for the EOD task. The system composes the following modules: 1) Taurus robot teleoperation system, 2) OECT device for detecting explosive residues, 3) TENG tactile sensor, 4) learning algorithms for object visualization, and 5) haptic display devices and controllers.

motion variability, and reduced time on task. Park et al. [54] also found that haptic feedback can significantly improve the performance during telerobotic locomotion and item exploration at an art museum. This system was applied as part of an assistive-technology-based interface for arts exploration. Both visually impaired and blindfolded sighted users experienced a reduction in task completion time and effort.

While haptic feedback can improve telerobotic navigation and exploration, the difference between the remote sense of touch and the actual tactile experience is vast. Controllers that provide force feedback can provide contact information for one or two interaction points, and they may also provide some proprioceptive information. Devices like Force Dimension's Omega series offer commercially available force feedback integrated with multi-DOF control [55]. However, human touch typically involves reception of a wide array of features not captured by this mechanism, including skin stretch, pressure, temperature, pain, weight, and texture [56]. Conveying these characteristics to the skin during teleoperation is a complex task, particularly when vision is not available. There are a number of technologies intended to convey some of these individual features existing in touch, such as TanvasTouch technology from [57], which uses friction modulation on a touchscreen to allow the finger to experience texture, as well as the Stretch-Pro from [58], which simulates the natural skin stretch associated with motor tasks of intact limbs for prosthetic users.

Another approach for conveying haptic information through robotics involves encoding that information and presenting it in a haptic modality that is more easily accessible and processed at the user's end. For example, with the current state-of-the-art teleoperation system, it is not possible to deliver a material tactile sensation immediately. However, material information can be encoded as vibration, then haptics can be used to convey such information to the operator in real time. Encoding information through vibrotactile stimuli also provides an opportunity to work around known limitations in tactile spatial resolution in order to achieve maximum information transfer [59]. Reed et al. [13] demonstrated that users can learn a high number of distinct vibrotactile codes given sufficient training. Their results indicate that users can learn to identify as many as 39 unique vibrotactile codes differentiated by properties such as frequency, location, duration, and apparent motion.

One other avenue by which haptic feedback can aid in teleoperation tasks is by cueing operators to notice key information on other modalities through specific signals, such as drawing attention to a relevant portion of a screen. Hameed et al. [60] demonstrated that haptic cues conveying the importance of an interrupting task were reliably interpreted by operators and were used by some to inform task switching.

E. Tactile Object Visualization

In teleoperation tasks, most tactile sensors can only characterize volumetric objects by sampling a partial observation per touch, which requires a sequence of observations to allow recognition of the object. Nevertheless, human operators have a limit in the memory capacity, which constrains the maximum number of features that can be recalled afterward [61]. As suggested by studies from [61] and [62], the pattern of features, and spatial relationship between them became inaccurate if the length of such contact sequences was beyond this limit. When such haptic exploration sequence is used for object recognition, the accuracy is not sufficiently high even if the exploration trajectories were frequently repeated [63]. This in turn, has a negative effect on the operator's situational awareness.

In this article, we introduce visual cues of contact locations that can be persistently visualized, aiming to reduce the memory capacity required by the exploration tasks. The visual cues have been previously applied to the field of telesurgery, which can improve the task performance when being integrated into the visual feedback [64]. Properly designed visual markers can improve the situation awareness of teleoperators [65], and mitigate

the negative effects when time delay exists [66]. When optical information is not available, the discrete contact points can be visualized by visual markers or as object models. Previous studies have shown that it is possible to align observations to its ground-truth model by pose estimation [67]. When the ground-truth object model is not available, it is possible to convert the points to surfaces by geometric learning techniques. One of the most common approaches is the Gaussian process implicit surface (GPIS) [68], which creates an implicit surface based on a sparse point set. The reconstructed results are smooth, with low noise, and of infinitely high resolution. The limitation of such reconstruction technique is that the result is constrained to be a watertight surface, which is not visually intuitive for representing incomplete object observations obtained when the exploration is ongoing. This issue can be addressed by incorporating the uGPIS algorithm proposed in our previous work [12].

III. System Architecture

A. System Description

The architecture of the proposed system is given in Fig. 2. The system consists of the following modules:

1) Taurus robot teleoperation system;
2) OECT chemical sensor;
3) TENG tactile sensor;
4) learning algorithms for object visualization;
5) haptic display devices and controllers.

These modules are described in Sections IV–VII. Such a system integration enables multimodal measurements and telepresence, which facilitates object characterization not only by optical cameras, but also by tactile sensors. The analyzed results from contact features, material characteristics are conveyed back to the teleoperator using haptic devices (Omega.7 controller, and vibrotactile sleeves) to enable improvements in operator's situational awareness and suitable maneuvers for explosive disposal. After the acquisition of contact samples, global properties of objects, such as shape and category can be determined to assist decision making.

B. Taurus Robot Teleoperation Platform

Taurus is a dexterous dual-arm teleoperation platform developed by SRI International. The robot is equipped with multiple sensory channels to improve a teleoperator's situational awareness. The robot has stereo cameras that can provide real-time visual feedback through TCP/IP communications. The visual stream is displayed to the teleoperator through a 3-D monitor, or optionally through VR headsets for an immersive teleoperation workspace. Second, the robot provides tactile feedback that enables interacting with objects safely. This is possible through interfacing the robot tooltip control with a pair of Omega.7 controllers (Force Dimension).

Tactile and haptic feedback to the operator is supported using two sources of force inference.

1) Slowly varying forces of less than 10 Hz are estimated by resolving the position error vector of the joints of the remote robot. With known stiffness, each error vector is converted into a tip force vector, which is subsequently transformed into the input device reference frame. Integral gains are disabled to permit joint position errors to be used as a proxy for joint torque measurements.
2) High-frequency (20–100 Hz) vibrations of the end effectors are measured using three-axis accelerometers, distally mounted on each arm. The tip accelerations are resolved into the input device coordinate system, through the camera system transformation. Then, these signals are superimposed as force waveforms on the haptic interface devices. A low-pass filter in the command signal chain prevents the controller motion from instability (caused by destabilizing feedback).

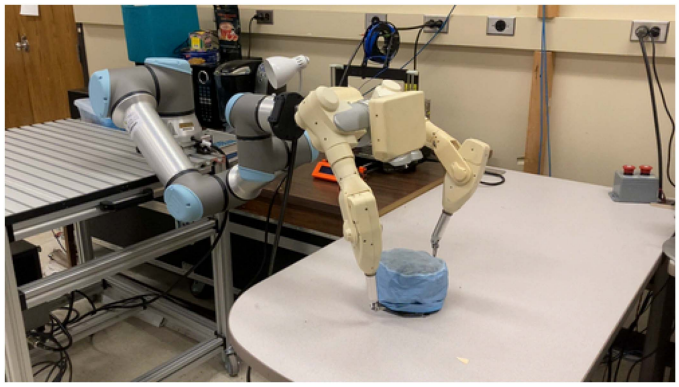

Fig. 3. Taurus telepresence platform mounted on a UR16e robot.

The bimanual movements are achieved by two 7-DOF arms. Each arm is equipped with an end effector that can perform object manipulation with high precision. The control system operates in position-to-position mode, where the remote manipulator joints are sent to new angles every 4 ms based on the transformed pose of the hand controllers. The tip pose is returned at the same update rate, and is used to calculate the tip position error vector. The joint level position control of the robot runs in a 2-kHz hardware loop. The left gripper has a dovetail adaptor, which allows tools to be mounted or changed during the operation. The tools needed by EOD operators include the wet swab for residue collection, and the TENG tactile sensor for object characterization.

To extend the physical operational volume range, the Taurus is mounted on a UR16e robot (Universal Robots), as shown in Fig. 3. The UR16e robot, in turn, is controlled by a remote computer using Real-Time Data Exchange protocol.

IV. Explosive Detection

EOD's effective decision making requires knowledge of the particular explosive needed to be disposed of. In these scenarios, improvised explosives will be the most prevalent and the ones that most urgently need to be detected. One approach for detection relies on the fact that many explosives utilize ammonium nitrate mixtures. Ammonium nitrate is readily soluble and dissociates in many common solvents producing a viable electrolyte. In this state, solution phase detection is accomplished using a

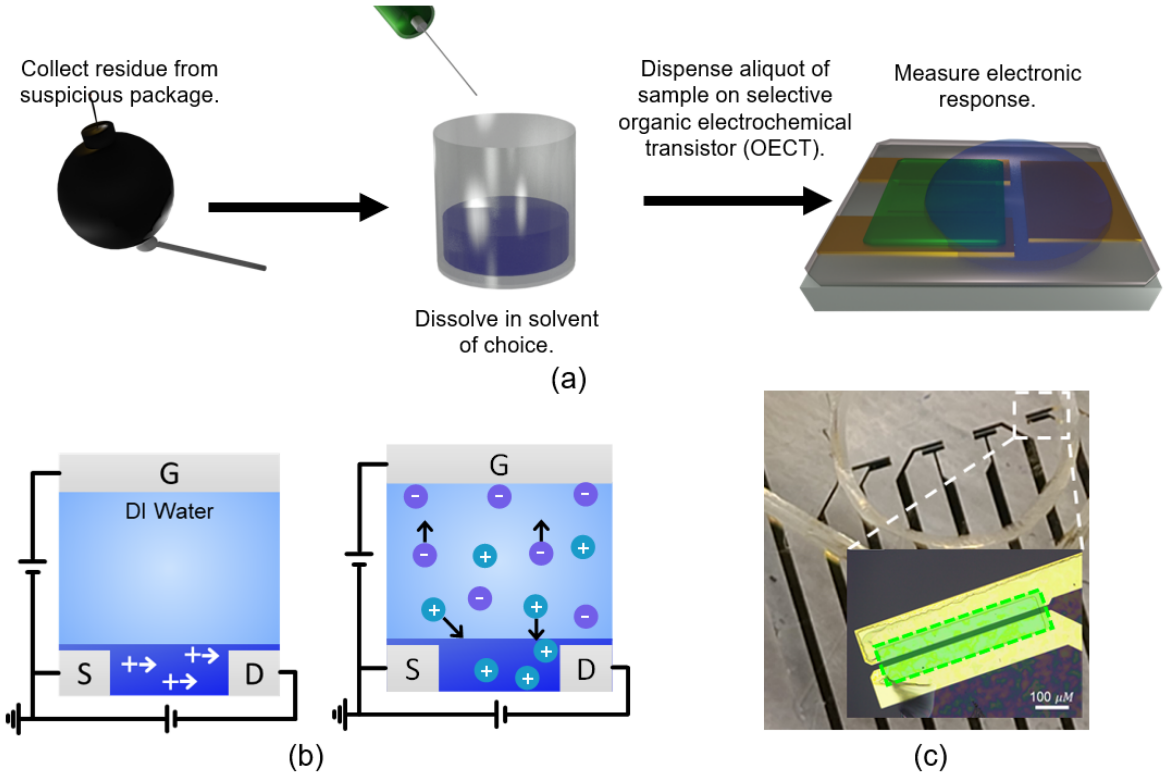

Fig. 4. (a) Schematic diagram depicting the proposed wet-swab sensing mechanism. In this process, residue is gathered using a swab which is subsequentially transferred and dissolved in a small stock solution. An aliquot of solution is transferred to the OECT for inspection. (b) Schematic illustration of PEDOT:PSS OECTs. When detecting ammonium nitrate, dissolved ions can penetrate the polymer blend and reversibly lower its conductivity monitored through drain current. (c) Photo of the demonstrative OECT device. The inset shows a microscope image of the sensing area (highlighted in green).

wet-swab inspection scheme, as shown in Fig. 4(a). Here in, a practical method for such detection requires the Taurus to swab a package of interest to collect residue using the tooltips and swabbing motion, and dissolve the residues in a reservoir of solvent for final characterization. Swabbing is an inexpensive and efficient means of collecting residue, making it ideal for remote ETD [69], [70]. An aliquot is siphoned and inspected using an OECT. Later, the OECT structure is generalized for detection of other explosives.

For ammonium nitrate detection, if the dissolved aliquot contains the salt, the applied voltage gate bias drives the explosive ingredient to intercalate into the organic channel and change the channel resistance [shown schematically in Fig. 4(c)]. The OECT sensor architecture allows a solution phase (rather than vapor phase) analysis bypassing the general concern of low vapor pressures in energetics [39]. Additionally, an individual OECT draws power under 1 W, is inexpensively prepared, and has an area less than 1 mm^2. A microscope image is given to highlight the sensing area. These properties allow us to utilize an array of OECTs operating in parallel to receive immediate chemical feedback on a variety of explosives.

Here, we demonstrate the operating principles in Fig. 4(c), which is applied to create a sensor sensitive enough to distinguish solutions containing various trace quantities of ammonium nitrate. These example OECTs employ a blend of poly(3,4-ethylene dioxythiophene) polymer doped with poly(styrene sulfonate) (PEDOT:PSS) for their channels. PEDOT:PSS is a common choice for OECT sensors and is commercially available making it a good channel material [34], [36], [37]. A photo of a real OECT device based on this principle is shown in Fig. 4(b).

OECTs were prepared on glass substrates fabricated with Au/Ti contacts and parylene insulation to produce channels with dimensions of 20 by 500 μm. 1.1 wt% PEDOT:PSS was purchased from Sigma Aldrich; added was 5 wt% ethylene glycol and trace 3-(glycidoxypropyl) trymethoxysiloxane and dodecylbenzene sulfonic acid. The PEDOT:PSS blend was spin-coated on the surface and annealed at 140 °C. Tested OECTs utilized silver/silver chloride pellet gate electrodes submerged in 100 μL of test solution (contained in a polydimethylsiloxane well) serving as an electrolyte gate. Solutions utilizing known concentrations of ammonium nitrate were prepared using high-performance liquid chromatography (HPLC) grade water, purchased from Sigma Aldrich, as a solvent. However, non-HPLC grade deionized water was used to dissolve swabbed residue. Sample surfaces were prepared by coating residue on copper sheets. Measurements were recorded using a Lakeshore probe station in tandem with a Keithley source meter controlled using LabTracer software.

V. Triboelectric Tactile Sensor

A. Working Mechanism of the TENG

The structure of the TENG device can be divided into two parts. The first part is called contact layer made of dielectric

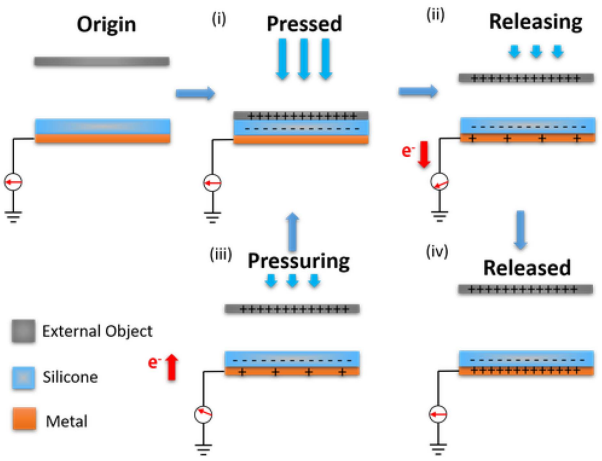

Fig. 5. TENG working mechanism.

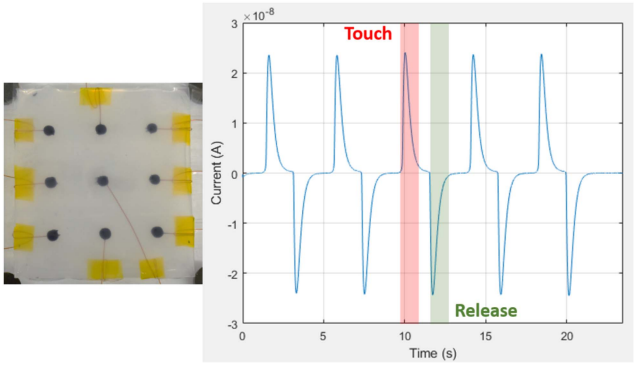

(a) (b)

Fig. 6. (a) TENG device (size at around 5 cm × 5 cm). (b) Electrical output of TENG under periodic physical contacts (sampled at 1000 Hz).

material such as silicone with a metal electrode on the other side. The second part is a counter layer, which is an external object that the TENG is about to approach. The basic working mechanism of TENG includes triboelectrification and electrostatic induction [71]. Fig. 5 illustrates a complete operation cycle for a TENG tactile sensor. When silicone and an external item come into contact under mechanical pressure [as seen in Fig. 5(i)], static charges may be generated on the contact region as a result of contact electrification. Given that TENG's structure may be compared to that of a precharged capacitor, the distance between TENG and the object surface is equivalent to the capacitance change. As a result, a charge flow can be created. This is depicted in Fig. 5(ii). Fig. 6 illustrates a typical TENG signal during one entire operating cycle. It comprises of a positive peak (red shadow) representing a contact event and a negative peak (green shadow) representing a contact-break event between the TENG and the external object.

The output voltage of TENG can be described as

$$V_{\text{oc}} = \frac{\sigma d}{\epsilon_0} \tag{1}$$

where d is the distance between TENG and the external object, σ is the surface charge density, and ϵ_0 is the relative permittivity of the contact layer.

Among these parameters, surface charge density is mainly determined by the intrinsic material properties as reported in the triboelectric series chart [72]. Any material's triboelectric series rank is determined by its tendency to gain or lose charges during the contact-separation step, which is shown in Fig. 5. The rank difference between the contact material from TENG and an external material determines the quantity of triboelectric charge generated, and hence, the output signal's magnitude, phase, and spectrum. This is the essential idea underlying material identification in tactile sensing based on TENGs.

The output of TENG is also positively proportional to the input pressure based on the previous reports [73], [74]. The reason can be attributed to the change of effective contact area, which alters the surface charge density shown in (1). The microlevel elastic deformation will lead to a more intimate contact under large pressure given that the stiffness of the contact layer (silicone) is relatively low. Compared with a conventional capacitive tactile sensor, TENG can directly establish force-sensitive behavior with no further modification on sensor itself or external circuit.

B. Device Fabrication

Based on the aforementioned working principle (see Section V-A), a prototype TENG trackpad with nine taxels [see Fig. 6(a)] is designed and fabricated by the following steps. First, the conductive electrode was printed onto the PCB board with a 3 × 3 array spatial layout. Carbon grease was applied as the electrode material due to its excellent conductivity and compatibility with the printing process. After that, a layer of silicone was cast-coated onto the PCB board to fully cover the as-printed electrode. This silicone layer is used as the dielectric layer, and also provides the protection for the electrodes. Given that the average height of the electrode was 3 mm, the thickness of the silicone layer was controlled to be 5 mm. The final step was to bake the whole device at 50 °C for 10 min using a hotplate.

VI. Object Visualization

Two methods are proposed to create visualization based on the collected tactile observations. The goal of using such visualization is to provide a reference to the user about where the contact locations are, so to reduce the cognitive load on the user. This is done by (appeared in our previous work [12], [15]): converting sparse tactile samples to a refined mesh model, and predicting the object label by a volumetric deep learning classifier.

A. Visual Rendering

It is possible to visualize the underlying surface of objects by creating the implicit surface from observed contact samples. We achieve this by first addressing the limitations of Gaussian process implicit surface (GPIS), which is an algorithm that was commonly adopted by previous studies for visualizing tactile sampled data [75], [76]. Given that the internal parts of objects are not reachable by direct touch, the truncated signed distant

field (TSDF) function required by the GPIS method cannot be directly measured by tactile sensors. While it is possible to use predicted TSDF function as a substitution, the prediction itself may not be accurate and may result in reconstruction failure.

The aforementioned challenges are tackled using the unsigned GPIS (uGPIS) algorithm proposed in our previous work [12]. To summarize, the uGPIS is used to reconstruct the surface using the occupancy possibility function $f_o(\cdot) \in [0, 1]$. The occupancy function is measured by the tactile sensor, which is defined as follows:

1) contact point set O with $f_o(\mathbf{x}_o) = 1$ for all $\mathbf{x}_o \in O$;
2) trajectory point set V that are within the free region of the space with $f_o(\mathbf{x}_v) = 0$ for all $\mathbf{x}_v \in V$.

Since we only focus on visualizing points that have been detected, a dummy point cloud grid U with $f_o(\mathbf{x}_u) = 0$ for all $\mathbf{x}_u \in U$ is created to fill those unobserved regions that are afar from the object (greater than a threshold distance d_s). Then, a Gaussian process with the radial basis function kernel is used for surface regression. The kernel parameters are learned by fitting on the training set that consists of all points in V, O, U, and the labels $f_o(\mathbf{x}_v)$, $f_o(\mathbf{x}_o)$, $f_o(\mathbf{x}_u)$ for each point set, respectively.

As an improvement to our previous work [12], the visualization is created by extracting a given number of iso-surfaces (K level set values), at an equal interval between the range of 5% and 95% percentile number of $(\hat{f}_o(\mathbf{x}_1), \hat{f}_o(\mathbf{x}_2), \ldots, \hat{f}_o(\mathbf{x}_n))$ for all $\mathbf{x_i} \in O$ (denoted as $[T_5, T_{95}]$). This is an improvement over our previous work [12] where now the percentile range is used as a filter to remove outliers that are difficult to be regressed. Using this approach improves the effect of visualization.

B. Object Recognition

Object recognition is used to assist the teleoperator, in order to understand the type of objects being touched. One problem is that the point cloud data collected from tactile sampling may have multifactorial variances. These variances are result of arbitrary object rotation, sparsity, measurement noise, etc. Such variances in the input data may affect the performance in most deep learning schemes. To tackle this issue, Triangle-Net, a deep neural network, which is robust toward multifactorial variances is applied [15].

Here, we briefly introduce the Triangle-Net model in [15]. The working principle is to learn on a representation that remains invariant to multifactorial variances. Rather than directly learning on point clouds, the input features to the network are triangle parameters generated by randomly selecting a given number of triads (denoted as $\mathscr{D}(\mathbf{x}_i, \mathbf{x}_j, \mathbf{x}_k)$) from the input point cloud. Note that using a fixed number of triads enables the network to tackle an arbitrary number of input points. Empirically, a greater number of triads contribute to higher accuracies at the cost of computational load. We found through experiments that using 4096 triads is sufficient for point clouds with a thousand or lower number of points. The entry of each feature includes triangle's edge distance, triangle's inner angle, angles between triangle edges and the contact force direction. Once the features are obtained, a deep neural network (denoted as H_Θ) is used to map the triangular features to a high-dimensional space. Last, all features are aggregated by a dimension-wise max function to obtain a latent vector. This process is represented as follows:

$$\mathscr{A}(\mathbf{x}_i) = \max_{i,j,k \in \mathscr{E}} H_\Theta\left(\mathscr{D}_m(\mathbf{x}_i, \mathbf{x}_j, \mathbf{x}_k)\right). \tag{2}$$

A classification network can be built upon the latent vector $\mathscr{A}(\mathbf{x}_i)$. In our implementation, both function H_Θ and the classification heads are chosen as multilayer perception networks. This design allows the network to be trained end-to-end by an optimizer, such as the Adam optimizer in our case [15].

Fig. 7. Photo of a participant wearing one tactile display on the upper left arm and the other on the right forearm (from [14]).

VII. Haptic Display

The data from the TENG sensor can be presented to the operator haptically. This approach offloads some information from the audio and visual channels allowing more cognitive resources on the operator side. Moreover, humans gather information for material categorization and pressure sensing haptically, so there is a natural motivation to continue to present that information via the skin even when mediated by a robotic system.

The display consists of two haptic sleeves, one worn on the forearm and the other on the opposite upper arm, as shown in Fig. 7. Different body sites were selected on the left and right arms to avoid misplacement errors of homologous locations (for example, see [77] and [78]). Each is comprised of an array of 12 tactors. This design aims to present categorical information (*i.e.*, discrete categories of materials or levels of pressure) thresholded from the continuous data produced by the TENG sensors.

The arms were selected as the display site due to their high tactile sensitivity and ease of access [56]. Compared to other areas sensitive to touch (face, fingers, and feet), the arms are more available for use during a teleoperation task. There is also a natural analogy between the two arms of the operator and the two end effectors of the Taurus robot. It would be possible to map the TENG signals from the right-end effector to the right arm and from the left-end effector to the left arm. The decision to use vibrotactile signals and discretize information such as contact pressure was motivated by the known limitations of control stability and force transparency in force feedback,

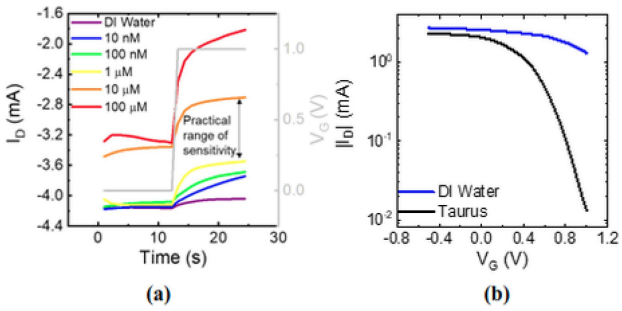

Fig. 8. (a) Preliminary results of OECTs tested using solutions of known ammonium nitrate concentration. (b) Results when the OECT was challenged by a solution containing residue gathered by swabbing with the Taurus (black), compared to the case where the device was challenged with ionized water (blue) used to collect residue.

as well as the research by Reed et al [13], demonstrating that participants could be trained to identify 39 unique vibrotactile signals encoding categorical information (English phonemes) with a mean recognition rate of 86%.

In order to determine the most effective encoding of material categories or pressure levels to vibrotactile signals, experiments were conducted to determine the selective attentional limitations of the system. These are described in Section VIII-C.

VIII. Experiments

A. Residue Detection

The first method of OECT testing measured the transient response produced by solutions of known ammonium nitrate concentration [see Fig. 8(a)]. A test device contained the analyte solution of interest to serve as an electrolyte gate. The gate voltage was, first, held at VG = 0 V, then, stepped the bias to VG = +1 V while measuring drain current, ID (using a constant source-drain bias of −0.5 V). The step change in gate bias produced a transient rise in current, ensuring a general response time of <30 s. Importantly, the OECT could analyze solutions with 1–10 μM ammonium nitrate concentrations. This concentration can be reached by collecting ∼1 μg of residue—a quantity that can be achieved via swabbing [69], [70]. Second, OECTs were tested using electrolytes prepared by swabbing residue from a surface [see Fig. 8(b)]. Specifically, ammonium nitrate was collected using the Taurus to swab a hard metal surface containing salt residue. The swabbing process required ∼90 s and collected enough residue to induce a two order of magnitude decrease in drain current, a reasonable timeframe for improvised explosive detection.

B. Characterization of the TENG Tactile Sensor

To study the pressure sensitivity of the TENG sensing unit, its electrical output as a function of loading forces was investigated. For copper material, the result is shown in Fig. 9(a). The electrical signal of the TENG increased in an approximately linear manner with increasing pressure between 9 and 250 kPa. The pressure sensitivity of the TENG unit is defined as $S = \frac{\Delta I}{Is \Delta P}$, where ΔP is the change of pressure, ΔI is the change of the

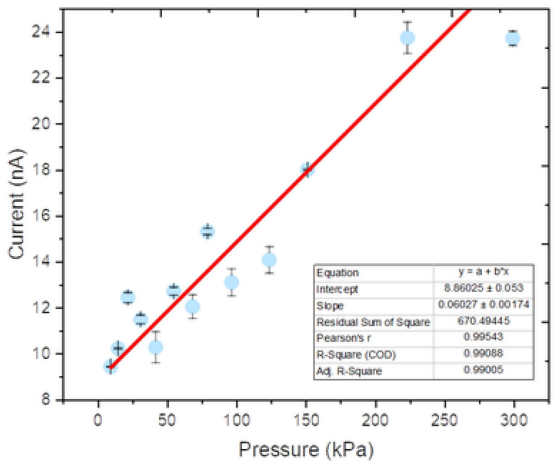

(a)

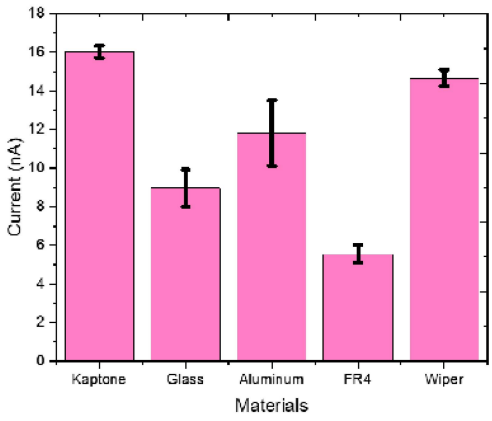

(b)

Fig. 9. (a) Relationship between the TENG electrical output and input pressure (red line: linear regression result). (b) Different TENG electrical output amplitude for various contact materials.

signal current resulting from the change in the pressure, and Is is the saturated current under the pressure test. The calculated sensitivity is around 2.7 Pa^{-1}, showing a promising performance for pressure sensing-related application.

When the pressure of the device was fixed at 60 kPa, the electrical response of the TENG with five different materials is shown in Fig. 9(b). There was a clear signal amplitude difference observed among these five materials. This indicates that the relative amplitude strength relationship could potentially provide a starting point for a material identification strategy.

C. Selective Attention to Haptic Stimuli

To map the tactile information to a haptic display, it was necessary to understand the number of discrete haptic signals the operator could reliably identify under various attentional conditions. An experiment was conducted to determine the attentional limitations of an operator when haptic stimuli were presented simultaneously on both arms (appeared earlier in [14]). Ten participants were trained and tested on identification of vibrotactile stimuli presented via the displays show in Fig. 7. Participants

were randomly assigned a nonsymmetric configuration of the displays, with one display worn on the left (right) forearm and the other worn on the right (left) upper arm. Nine distinct vibrotactile stimuli were employed in the study, characterized by a combination of location on the tactor array (dorsal distal, volar middle, or dorsal proximal) and frequency (300 Hz, 60 Hz, or 300 Hz with 60-Hz amplitude modulation). All stimuli were presented at 25 dB above the participant's detection threshold.

First, participants were allowed to train by freely playing the nine stimuli or using self-testing with feedback. After training, participants completed five sessions of testing across five days. For each session, five conditions were tested for one 100-trial run each, for a total of 2500 trials per participant. The conditions were: left arm stimulated, left arm attended (L, L); right arm stimulated, right arm attended (R, R); both arms stimulated, left arm attended (LR, L); both arms stimulated, right arm attended (LR, R); and both arms stimulated, both arms attended (LR, LR). The order of these five conditions was randomized for each session.

Participants demonstrated evidence of an ability to selectively attend to stimuli on a certain arm, with particularly strong performance for location information. Average percent-correct (pc) scores were calculated across all runs and participants. Statistically significant differences were found between the results of the single-arm conditions ($avg = 92\%$), selective attention conditions ($avg = 82\%$), and divided attention condition (50%). The slight decreasing trend seems primarily attributable to performance for frequency identification, as average pc scores for location information only were notably high across all conditions, both for the undivided attention conditions, (L, L), (R, R), (LR, L), and (LR, R) ($avg = 98\%$), and the divided attention condition (85%). Information transfer (IT) estimates suggest that using six alternatives (three location alternatives and two frequency alternatives) could allow participants to perform highly under selective attention conditions. The IT results also indicate that participants could identify 24 combinations of left/right arm, location, and frequency information.

The results of this study indicate that as many as 24 categories of information from the tactile sensor can be reliably identified by an EOD operator. Knowing the selective attentional limitations of this system allows us to offload the contact information from the visual modality. Being able to display contact information simultaneously on both arms could also enable tactile object exploration with both end effectors.

D. Augmented Tactile Visualization

Experiments were conducted to create augmented visualizations based on tactile samples. For this, a simulation was created to collect tactile samples from virtual objects. This experiment appeared in [12]. A human teleoperator was involved in the experiment by controlling the position of a simulated tactile sensor. The control command, together with the produced force when interacting with objects, were transmitted bidirectionally by an Omega. 7 haptic device (Force Dimension). In Fig. 10, the reconstructed surfaces for three virtual objects are demonstrated: a banana, a bowl, and a scissor. It can be seen that the shape of the reconstructed isosurface is consistent with the groundtruth object and the point priors as well. Moreover, the robustness of the reconstruction process was demonstrated when the sampled points only cover a partial region of the object, showing that reasonable reconstruction results can still be obtained even if the objects does not hold the watertight assumption.

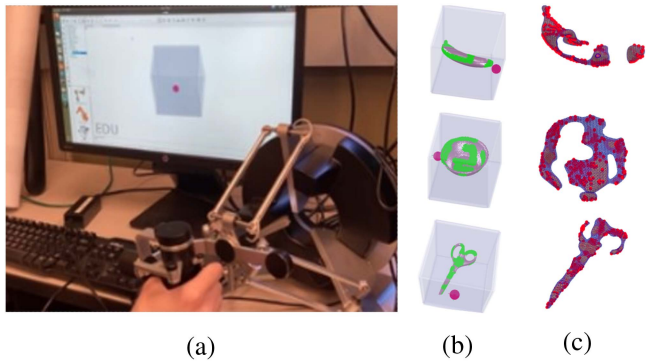

Fig. 10. (a) Simulation for obtaining point samples. (b) Example of objects, and the region covered by contacts point clouds (green). (c) Isosurface from augmentation.

Recognizing corrupted tactile samples can increase operator's cognitive load. Therefore, the predicted object type is displayed as an assistant approach. This is implemented by leveraging a point cloud recognition network Triangle-Net [15], which achieved satisfactory accuracies in both human-guided tactile exploration dataset and corrupted virtual object datasets. In our previous work [15], experiments were conducted on a highly corrupted ModelNet 40 dataset [79], which has 40 categories with 12 311 CAD models in total. All the objects were downsampled to 16 points per object and are rotated by arbitrary SO(3) transformation around the center. Under such an extreme corrupted condition, the Triangle-Net achieved 70.35% top-1 accuracy. In comparison, the PointNet model only achieved 35.28% due to the combined variations from the unknown object pose and the sparsity [15].

In our previous study [12], evaluations were conducted using human-guided tactile sampling data in a simulated environment. Triangle-Net [15] achieved a 76.7% top-five classification accuracy using the collected contact points from the simulated tactile exploration environment, while the baseline algorithms PointNet [80] and DGCNN [81] only achieved 38.4% and 39.7% top-five accuracy, respectively. Future work includes conducting a systematical human subject study, in order to evaluate on recognizing samples from concealed objects by the real Taurus robot. The study will focus on human performance in teleoperation situations. An example is to compare human's object recognition accuracy without assistance, to situations with assistance information available to the user (predicted shape and object category information).

IX. Discussions

Our work thus far has focused on developing a series of technologies for IED characterization using the Taurus teleoperated robot. While the purpose of this article is to showcase

the functional module of each part, we anticipate the system could be integrated in the following ways. First, a more compact tactile sensor needs to be developed to facilitate integration with Taurus gripper. The new tactile sensors will need to be small enough to be carried by the Taurus dovetail adapter. Its feedback channels need to be integrated into the robot's communication protocols. A compact design of haptic sleeves could allow for ease of use by the teleoperator without affecting the user's hand dexterity. In addition, we plan to develop a swabbing tool for residue collection that can be carried by the robot. Preliminary studies have shown that designs similar to whisker filaments may be suitable for this application, as they allow for conformal swabbing of surfaces while being minimally intrusive to the object surface.

The tactile feedback from the Taurus robot gripper is necessary for safe teleoperation, as it provides information about the contact force direction and high-frequency vibration signals that are critical to haptics rendering through Omega.7 controllers. Nevertheless, it is still not sensitive enough for contact detection in a minimally intrusive way. In comparison, the TENG sensor may allow for highly sensitive contact detection and characterization. Further, the TENG sensor also allows for the discrimination of the materials and the applied pressure, which can be achieved through interpreting the information (e.g., pulse shape, rise/fall time, etc.) from the original triboelectric waveforms leveraging machine learning approaches. The current work establishes a platform to explore more complex problems such as using tactile signals to help visualize the properties of the objects (e.g., surface, materials, etc.). The demonstration of the capability to identify and discriminate different materials warrants more comprehensive follow-up efforts. One interesting direction is conveying material information (e.g. category) to the operator using haptics in real-time, in addition to informing about contact events only. This can be achieved through mapping different material categories detected by TENG sensor to different body sites using haptics sleeves.

Conducting human subjects studies would be a necessary step in building such an integrated system. We plan to systematically conduct evaluations on a series of tasks, such as simulated IED material analysis through a TENG sensor, residue collection and composition analysis through OECT sensor, and performing mechanical separation of simulated IED devices through robot manipulation.

X. Conclusion

In this article, we investigated a suite of techniques for a tactile-based EOD robot, aiming to mitigate the risk from deadly scenarios. Compared to conventional EOD robots, the proposed techniques allowed us to extend the application of EOD robots to scenarios where visual information cannot provide sufficient situational awareness for successful task execution. In the described system, we leveraged the Taurus robot, which was controlled remotely through teleoperation. To identify the risk, an OECT device was designed to search for the occurrence of explosive residues. By having this information, the risk can be assessed in advance, and precautionary actions can be undertaken to prevent further harm, or disengagement maneuvers can be executed. Safe interaction with suspicious objects was accomplished by the combination of tactile sensors and haptic display devices, allowing users to get real-time force feedback and multimodal information for object characterization. The accumulated evidence, in the form of observations from suspicious objects, could be visualized to enable an intuitive understanding of the environment and to increase situational awareness. Because of the number and complexity of simultaneous tasks that the EOD operator was required to perform, an experiment was conducted to determine the attentional limitations of the users. Future work includes an experiment that will involve the transmission of more complex semantic information using the aforementioned vibrotactile sleeves, such as contact events, texture cues, and alert levels identified from the explosive residues.

The main outcomes of this work were the ability to recognize the type of explosive residues by a quantity that can be achieved by swabbing (around 1 μg), triboelectric tactile sensor that were capable of conveying pressure and material type, highly robust deep learning methods that can recognize object category from contact samples with multifactoral disturbances (only requires 8–16 points per object), and haptic/visual rendering methods that can provide the navigational guidance. Future work will include the integration of the proposed technologies into the Taurus manipulation platform for simulated IED characterization tasks or disassembly procedures, and render the semantic information from the TENG and OECT devices through haptic devices.

Acknowledgment

The authors would like to thank M. Wu for the help on testing the tactile sensor. This work involved human subjects in its research. Any opinions, findings, and conclusions or recommendations expressed in this material are those of the author(s) and do not necessarily reflect the views of the National Science Foundation.

References

[1] J. L. Otto et al., "Explosive ordnance disposal personnel in the US military have higher risk of insomnia and post-traumatic stress disorder: A large retrospective cohort study," *Ann. Epidemiol.*, vol. 57, pp. 40–45, 2021.

[2] P. J. Patel, G. A. Gilde, P. G. Dehmer, and J. W. McCauley, "Transparent ceramics for armor and em window applications," *Proc. SPIE*, vol. 4102, pp. 1–14, 2000.

[3] C. Bass et al., "A methodology for assessing blast protection in explosive ordnance disposal bomb suits," *Int. J. Occup. Saf. Ergonom.*, vol. 11, no. 4, pp. 347–361, 2005.

[4] Y.-N. Wu et al., "Characterizing the effects of explosive ordnance disposal operations on the human body while wearing heavy personal protective equipment," *Hum. Factors*, vol. 64, no. 7, 2021, Art. no. 0018720821992623.

[5] D. Ryu, S. Kang, M. Kim, and J.-B. Song, "Multi-modal user interface for teleoperation of ROBHAZ-DT2 field robot system," in *Proc. IEEE/RSJ Int. Conf. Intell. Robots Syst.*, 2004, vol. 1, pp. 168–173.

[6] M. W. Carey, E. M. Kurz, J. D. Matte, T. D. Perrault, and T. Padir, "Novel EOD robot design with dexterous gripper and intuitive teleoperation," in *Proc. World Automat. Congr.*, 2012, 2012, pp. 1–6.

[7] D. B. Kaber, E. Onal, and M. R. Endsley, "Design of automation for telerobots and the effect on performance, operator situation awareness, and subjective workload," *Hum. Factors Ergonom. Manuf. Serv. Industries*, vol. 10, no. 4, pp. 409–430, 2000.

[8] A. J. Burtness, "Evaluation of haptic feedback methods for teleoperated explosive ordnance disposal robots," Ph.D. dissertation, Johns Hopkins Univ., Baltimore, MD, USA, 2011.

[9] A. Kron, G. Schmidt, B. Petzold, M. I. Zah, P. Hinterseer, and E. Steinbach, "Disposal of explosive ordnances by use of a bimanual haptic telepresence system," in *Proc. IEEE Int. Conf. Robot. Automat.*, 2004, pp. 1968–1973.

[10] T. Yamamoto, M. Bernhardt, A. Peer, M. Buss, and A. M. Okamura, "Techniques for environment parameter estimation during telemanipulation," in *Proc. IEEE 2nd RAS EMBS Int. Conf. Biomed. Robot. Biomechatron.*, 2008, pp. 217–223.

[11] E. P. Westebring-van der Putten, R. H. Goossens, J. J. Jakimowicz, and J. Dankelman, "Haptics in minimally invasive surgery—A review," *Minimally Invasive Ther. Allied Technol.*, vol. 17, no. 1, pp. 3–16, 2008.

[12] C. Xiao, N. Madapana, and J. Wachs, "Fingers see things differently (FIST-D): An object aware visualization and manipulation framework based on tactile observations," *IEEE Robot. Automat. Lett.*, vol. 6, no. 3, pp. 4249–4256, Jul. 2021.

[13] C. M. Reed et al., "A phonemic-based tactile display for speech communication," *IEEE Trans. Haptics*, vol. 12, no. 1, pp. 2–17, Jan.–Mar. 2019.

[14] G. M. Clepper, J. S. Martinez, and H. Z. Tan, "Selective and divided attention for vibrotactile stimuli on both arms," in *Proc. IEEE World Haptics Conf.*, 2021, pp. 650–655, doi: 10.1109/WHC49131.2021.9517140.

[15] C. Xiao and J. Wachs, "Triangle-Net: Towards robustness in point cloud learning," in *Proc. IEEE/CVF Winter Conf. Appl. Comput. Vis.*, 2021, pp. 826–835.

[16] M. Prem, M. E. Purroy, and J. F. Vargas, "Landmines: The local effects of demining," Jan. 27, 2023. [Online]. Available: https://ssrn.com/abstract=3924929

[17] M. Krausa, *Vapour and Trace Detection of Explosives for Anti-Terrorism Purposes*, vol. 167. Berlin, Germany: Springer, 2004.

[18] S. Cheng et al., "Dopant-assisted negative photoionization ion mobility spectrometry for sensitive detection of explosives," *Anal. Chem.*, vol. 85, no. 1, pp. 319–326, 2013.

[19] L. Lazarowski and D. C. Dorman, "Explosives detection by military working dogs: Olfactory generalization from components to mixtures," *Appl. Animal Behav. Sci.*, vol. 151, pp. 84–93, 2014.

[20] J. Yinon, "Detection of explosives by electronic noses," *Anal. Chem.*, vol. 75, pp. 99–105, 2003.

[21] K. C. To, S. Ben-Jaber, and I. P. Parkin, "Recent developments in the field of explosive trace detection," *ACS nano*, vol. 14, no. 9, pp. 10804–10833, 2020.

[22] J. S. Caygill, F. Davis, and S. P. Higson, "Current trends in explosive detection techniques," *Talanta*, vol. 88, pp. 14–29, 2012.

[23] S. J. Toal and W. C. Trogler, "Polymer sensors for nitroaromatic explosives detection," *J. Mater. Chem.*, vol. 16, no. 28, pp. 2871–2883, 2006.

[24] United States Bomb Data Center Explosives Incident report, *Bur. Alcohol, Tobacco, Firearms, Explosives*, Washington DC, USA, Tech. Rep., 2020. [Online]. Available: https://www.atf.gov/explosives/docs/report/2014-usbdc-explosive-incident-report/download

[25] The National Academies, "IED attack: Improvised explosive devices," U.S. Department of Homeland Security, Tech. Rep., 2005.

[26] P. Li, X. Li, and W. Chen, "Recent advances in electrochemical sensors for the detection of 2, 4, 6-trinitrotoluene," *Current Opinion in Electrochemistry*, vol. 17, pp. 16–22, 2019.

[27] H. A. Yu, D. A. DeTata, S. W. Lewis, and D. S. Silvester, "Recent developments in the electrochemical detection of explosives: Towards field-deployable devices for forensic science," *TrAC Trends Anal. Chem.*, vol. 97, pp. 374–384, 2017.

[28] V. Krivitsky, B. Filanovsky, V. Naddaka, and F. Patolsky, "Direct and selective electrochemical vapor trace detection of organic peroxide explosives via surface decoration," *Anal. Chem.*, vol. 91, no. 8, pp. 5323–5330, 2019.

[29] M. Pesavento, G. D'Agostino, G. Alberti, R. Biesuz, and D. Merli, "Voltammetric platform for detection of 2,4,6-trinitrotoluene based on a molecularly imprinted polymer," *Anal. Bioanalytical Chem.*, vol. 405, pp. 3559–3570, 2013.

[30] J. Rivnay, S. Inal, A. Salleo, R. M. Owens, M. Berggren, and G. G. Malliaras, "Organic electrochemical transistors," *Nature Rev. Mater.*, vol. 3, no. 2, pp. 1–14, 2018.

[31] D. A. Bernards and G. G. Malliaras, "Steady-state and transient behavior of organic electrochemical transistors," *Adv. Funct. Mater.*, vol. 17, no. 17, pp. 3538–3544, 2007.

[32] V. Kaphle, P. R. Paudel, D. Dahal, R. K. Radha Krishnan, and B. Lüssem, "Finding the equilibrium of organic electrochemical transistors," *Nature Commun.*, vol. 11, no. 1, 2020, Art. no. 2515.

[33] J. Rivnay et al., "High-performance transistors for bioelectronics through tuning of channel thickness," *Sci. Adv.*, vol. 1, no. 4, 2015, Art. no. e1400251.

[34] J. Liao, H. Si, X. Zhang, and S. Lin, "Functional sensing interfaces of PEDOT:PSS organic electrochemical transistors for chemical and biological sensors: A mini review," *Sensors*, vol. 19, no. 2, 2019, Art. no. 218.

[35] O. Parlak, S. T. Keene, A. Marais, V. F. Curto, and A. Salleo, "Molecularly selective nanoporous membrane-based wearable organic electrochemical device for noninvasive cortisol sensing," *Sci. Adv.*, vol. 4, no. 7, 2018, Art. no. eaar2904.

[36] P. Lin, X. Luo, I. M. Hsing, and F. Yan, "Organic electrochemical transistors integrated in flexible microfluidic systems and used for label-free DNA sensing," *Adv. Mater.*, vol. 23, no. 35, pp. 4035–4040, 2011.

[37] X. Ji et al., "Highly sensitive metabolite biosensor based on organic electrochemical transistor integrated with microfluidic channel and Poly(N-vinyl-2-pyrrolidone)-Capped platinum nanoparticles," *Adv. Mater. Technol.*, vol. 1, no. 5, 2016, Art. no. 1600042.

[38] H. Tang, F. Yan, P. Lin, J. Xu, and H. L. Chan, "Highly sensitive glucose biosensors based on organic electrochemical transistors using platinum gate electrodes modified with enzyme and nanomaterials," *Adv. Funct. Mater.*, vol. 21, no. 12, pp. 2264–2272, 2011.

[39] H. Östmark, S. Wallin, and H. G. Ang, "Vapor pressure of explosives: A critical review," *Propellants, Explosives, Pyrotechnics*, vol. 37, no. 1, pp. 12–23, 2012.

[40] P. Wells and D. Deguire, "TALON: A universal unmanned ground vehicle platform, enabling the mission to be the focus," *Proc. SPIE*, vol. 5804, pp. 747–757, 2005.

[41] B. M. Yamauchi, "Packbot: A versatile platform for military robotics," *Proc. SPIE*, vol. 5422, pp. 228–237, 2004.

[42] G. De Cubber, H. Balta, and C. Lietart, "Teodor: A semi-autonomous search and rescue and demining robot," in *Applied Mechanics and Materials*, vol. 658. Bäch, Switzerland: Trans Tech Pub. Ltd., 2014, pp. 599–605.

[43] P. G. De Santos, J. A. Cobano, E. Garcia, J. Estremera, and M. Armada, "A six-legged robot-based system for humanitarian demining missions," *Mechatronics*, vol. 17, no. 8, pp. 417–430, 2007.

[44] O. Tavsel, "Mechatronic design of an explosive ordnance disposal robot," Master's thesis, Izmir Inst. Technol., Urla, Turkey, 2005.

[45] Z. Jian-Jun, Y. Ru-Qing, Z. Wei-Jun, W. Xin-Hua, and Q. Jun, "Research on semi-automatic bomb fetching for an EOD robot," *Int. J. Adv. Robot. Syst.*, vol. 4, no. 2, pp. 247–252, 2007.

[46] R. R. Murphy, J. Peschel, C. Arnett, and D. Martin, "Projected needs for robot-assisted chemical, biological, radiological, or nuclear (CBRN) incidents," in *Proc. IEEE Int. Symp. Saf., Secur., Rescue Robot.*, 2012, pp. 1–4.

[47] S. Kang et al., "ROBHAZ-DT2: Design and integration of passive double tracked mobile manipulator system for explosive ordnance disposal," in *Proc. IEEE/RSJ Int. Conf. Intell. Robots Syst.*, 2003, vol. 3, pp. 2624–2629.

[48] S. Nahavandi, J. Mullins, M. Fielding, H. Abdi, and Z. Najdovski, "Countering improvised explosive devices through a multi-point haptic teleoperation system," in *Proc. IEEE Int. Symp. Syst. Eng.*, 2015, pp. 190–197.

[49] J. Wormley et al., "High dexterity robotics for safety and emergency response-17104," WM Symposia, Inc., Tempe, AZ, USA, Tech. Rep. INIS-US-19-WM-17104 TRN: US19V0192038734, 2017.

[50] C. C. Kemp, A. Edsinger, and E. Torres-Jara, "Challenges for robot manipulation in human environments [grand challenges of robotics]," *IEEE Robot. Automat. Mag.*, vol. 14, no. 1, pp. 20–29, Mar. 2007.

[51] J. Rao et al., "Tactile electronic skin to simultaneously detect and distinguish between temperature and pressure based on a triboelectric nanogenerator," *Nano Energy*, vol. 75, 2020, Art. no. 105073.

[52] L. Lin et al., "Triboelectric active sensor array for self-powered static and dynamic pressure detection and tactile imaging," *ACS Nano*, vol. 7, no. 9, pp. 8266–8274, 2013.

[53] H. Tappeiner, R. Klatzky, P. Rowe, J. Pedersen, and R. Hollis, "Bimanual haptic teleoperation for discovering and uncovering buried objects," in *Proc. IEEE Int. Conf. Robot. Automat.*, 2013, pp. 2380–2385.

[54] C. H. Park, E.-S. Ryu, and A. M. Howard, "Telerobotic haptic exploration in art galleries and museums for individuals with visual impairments," *IEEE Trans. Haptics*, vol. 8, no. 3, pp. 327–338, Jul.–Sep. 2015.

[55] Force Dimension, omega.x, 2021. [Online]. Available: https://www.forcedimension.com/products/omega

[56] J. M. Wolfe et al., *Sensation & Perception*. Sunderland, MA, USA: Sinauer, 2006.

[57] E. Colgate, "Touching with feeling: Integrating haptics with touch displays," in *Proc. 25th Int. Display Workshops*, 2018, pp. 4–5.

[58] N. Colella, M. Bianchi, G. Grioli, A. Bicchi, and M. G. Catalano, "A novel skin-stretch haptic device for intuitive control of robotic prostheses and avatars," *IEEE Robot. Automat. Lett.*, vol. 4, no. 2, pp. 1572–1579, Apr. 2019.

[59] D. T. Pawluk, R. J. Adams, and R. Kitada, "Designing haptic assistive technology for individuals who are blind or visually impaired," *IEEE Trans. Haptics*, vol. 8, no. 3, pp. 258–278, Jul.–Sep. 2015.

[60] S. Hameed, T. Ferris, S. Jayaraman, and N. Sarter, "Supporting interruption management through informative tactile and peripheral visual cues," in *Proc. Hum. Factors Ergonom. Soc. Annu. Meeting*, 2006, pp. 376–380.

[61] M. Driels and P. Beierl, "A finite memory model for haptic teleoperation," *IEEE Trans. Syst., Man, Cybern.*, vol. 24, no. 4, pp. 690–698, Apr. 1994.

[62] M. Driels and D. Klein, "Combined visual and haptic search of remote object identification," in *Telemanipulator Technology*, vol. 1833. Bellingham, WA, USA: SPIE, 1993, pp. 220–227.

[63] T. Zhang, B. S. Duerstock, and J. P. Wachs, "Multimodal perception of histological images for persons who are blind or visually impaired," *ACM Trans. Accessible Comput.*, vol. 9, no. 3, pp. 1–27, 2017.

[64] L. Tanzi, P. Piazzolla, F. Porpiglia, and E. Vezzetti, "Real-time deep learning semantic segmentation during intra-operative surgery for 3D augmented reality assistance," *Int. J. Comput. Assist. Radiol. Surg.*, vol. 16, no. 9, pp. 1435–1445, 2021.

[65] B. Rosa et al., "Intuitive teleoperation of active catheters for endovascular surgery," in *Proc. IEEE/RSJ Int. Conf. Intell. Robots Syst.*, 2015, pp. 2617–2624.

[66] F. Richter, Y. Zhang, Y. Zhi, R. K. Orosco, and M. C. Yip, "Augmented reality predictive displays to help mitigate the effects of delayed telesurgery," in *Proc. IEEE Int. Conf. Robot. Automat.*, 2019, pp. 444–450.

[67] M. L. Villalonga et al., "Tactile object pose estimation from the first touch with geometric contact rendering," in *Proc. Conf. Robot Learn.*, Jan. 2020, pp. 1015–1029.

[68] O. Williams and A. Fitzgibbon, "Gaussian process implicit surfaces," *Gaussian Process Pract.*, pp. 1–4, 2006.

[69] J. M. E. Glackin et al., "Explosives detection by swabbing for improvised explosive devices," *Analyst*, vol. 17, pp. 7956–7963, 2020.

[70] J. S. Laster, C. D. Ezeamaku, S. P. Beaudoin, and B. W. Boudouris, "Impact of surface chemistry on the adhesion of an energetic small molecule to a conducting polymer surface," *Colloids Surfaces A, Physicochem. Eng. Aspects*, vol. 551, pp. 74–80, 2018.

[71] F.-R. Fan, Z.-Q. Tian, and Z. L. Wang, "Flexible triboelectric generator," *Nano Energy*, vol. 1, no. 2, pp. 328–334, 2012.

[72] H. Zou et al., "Quantifying the triboelectric series," *Nature Commun.*, vol. 10, no. 1, pp. 1–9, 2019.

[73] L. Wang et al., "A metal-electrode-free, fully integrated, soft triboelectric sensor array for self-powered tactile sensing," *Microsyst. Nanoeng.*, vol. 6, no. 1, pp. 1–9, 2020.

[74] X. Pu et al., "Ultrastretchable, transparent triboelectric nanogenerator as electronic skin for biomechanical energy harvesting and tactile sensing," *Sci. Adv.*, vol. 3, no. 5, 2017, Art. no. e1700015.

[75] D. Driess, P. Englert, and M. Toussaint, "Active learning with query paths for tactile object shape exploration," in *Proc. IEEE/RSJ Int. Conf. Intell. Robots Syst.*, 2017, pp. 65–72.

[76] C. Rosales, F. Spinelli, M. Gabiccini, C. Zito, and J. L. Wyatt, "GPAtlasRRT: A local tactile exploration planner for recovering the shape of novel objects," *Int. J. Humanoid Robot.*, vol. 15, no. 01, 2018, Art. no. 1850014.

[77] F. A. Geldard, "Cutaneous coding of optical signals: The optohapt," *Percep. Psychophys.*, vol. 1, no. 11, pp. 377–381, 1966.

[78] A. Gallace, H. Z. Tan, and C. Spence, "Numerosity judgments for tactile stimuli distributed over the body surface," *Perception*, vol. 35, no. 2, pp. 247–266, 2006.

[79] Z. Wu et al., "3D shapenets: A deep representation for volumetric shapes," in *Proc. IEEE Conf. Comput. Vis. pattern Recognit.*, 2015, pp. 1912–1920.

[80] C. R. Qi, H. Su, K. Mo, and L. J. Guibas, "PointNet: Deep learning on point sets for 3D classification and segmentation," in *Proc. IEEE Conf. Comput. Vis. Pattern Recognit.*, 2017, pp. 652–660.

[81] Y. Wang, Y. Sun, Z. Liu, S. E. Sarma, M. M. Bronstein, and J. M. Solomon, "Dynamic graph CNN for learning on point clouds," *ACM Trans. Graph.*, vol. 38, no. 5, pp. 1–12, 2019.

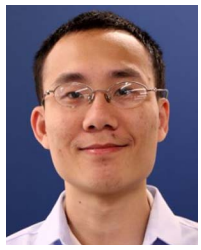

Chenxi Xiao (Member, IEEE) received the B.S. and M.S. degrees in electrical engineering from Northwestern Polytechnical University, Xi'an, China, in 2013 and 2016, respectively, and the Ph.D. degree in industrial engineering from Purdue University, West Lafayette, IN, USA, in 2003.

He had worked as a Research Assistant with the Intelligent Systems and Assistive Technologies (ISAT) Lab, Purdue University, advised by Prof. Juan P. Wachs. His research interests include robot tactile sensing and manipulation, motion planning, and artificial intelligence.

Aaron Benjamin Woeppel received the Bachelor in Science degree in chemical engineering from the University of Pittsburgh, Pittsburgh, PA, USA, in 2019.

He is currently serving as a Graduate Research Assistant and Fellow with the Davidson School of Chemical Engineering, Purdue University, West Lafayette, IN, USA. His research interests include incorporating polymers and soft materials into national security challenges. His main research interest is to utilize conductive polymers for detection of explosives.

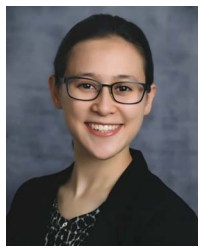

Gina Marie Clepper (Member, IEEE) received the B.S. degree in electrical engineering and the M.S. degree in electrical and computer engineering from Purdue University, West Lafayette, IN, USA, in 2019 and 2021, respectively.

She is currently in Columbus, OH, USA, where she designs interactive tactile graphics.

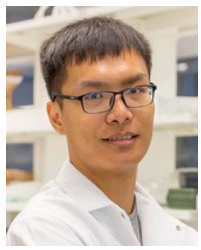

Shengjie Gao received the B.S. degree in materials chemistry from Lanzhou University, Lanzhou, China, in 2016, and the Ph.D. degree in industrial engineering from Purdue University, West Lafayette, IN, USA, under the supervision of Prof. W. Wu, in 2021.

His research interests include the piezotronics, self-powered system, and human–machine interface.

Shujia Xu received the B.S. degree in mechanical engineering form the South China University of Technology, Guangzhou, China, in 2015, and the M.S. degree in biomedical engineering from Sun Yat-Sen University, Guangzhou, in 2018. He is currently working toward the Ph.D. degree in industrial engineering with Purdue University, West Lafayette, IN, USA, under the supervision of Prof. W. Wu.

His research interests include materials and manufacturing innovations of triboelectric nanogenerators, and wearable electronics for human-integrated applications.

Johannes F. Rueschen received the B.S. degree in mechanical engineering from the Osnabrueck University of Applied Sciences, Osnabrueck, Germany, in 2019. He studied mechanical engineering with Leibniz University Hannover, Hannover, Germany and received the M.S. degree in mechanical engineering from Purdue University, West Lafayette, IN, USA, in 2020.

As a Graduate Researcher with the Haptic Interface Research Laboratory, Purdue University, he investigated the science and technology of displaying information through the sense of touch.

Daniel Kruse received the B.S. degree in electrical engineering from Virginia Commonwealth University, Richmond, VA, USA, and the M.S. and Ph.D. degrees in electrical engineering from Toyota Research Institute, Los Altos, CA, USA, in 2011 and 2016, respectively.

He previously worked with SRI International as a Senior Controls Engineer and is currently a Senior Research Scientist with Toyota Research Institute working on robotics for human amplification in real environments. His research interests include full body robot control and bridging the gap between human and robot behaviors.

Wenzhuo Wu (Senior Member, IEEE) received the B.S. degree in electrical engineering from the University of Science and Technology of China, Hefei, China, in 2005, the M.E. degree in electrical and computer engineering from the National University of Singapore, Singapore, in 2008, and the Ph.D. degree in materials science and engineering from the Georgia Institute of Technology, Atlanta, GA, USA, in 2013.

He is currently the Ravi and Eleanor Talwar Rising Star Associate Professor with the School of Industrial Engineering, Purdue University, West Lafayette, IN, USA. His research interests include the design, manufacturing, and integration of nanomaterials for applications in energy, electronics, optoelectronics, and wearable devices.

Hong Z. Tan (Fellow, IEEE) received the B.S. degree in biomedical engineering from Shanghai Jiao Tong University, Shanghai, China, in 1986, and the S.M. and Ph.D. degrees, both in electrical engineering and computer science, from the Massachusetts Institute of Technology, Cambridge, MA, USA, in 1988 and 1996, respectively.

She is currently the Keysight Professor of electrical and computer engineering with Purdue University, West Lafayette, IN, USA, with courtesy appointments in mechanical engineering and psychological sciences. She investigates the science and technology of displaying information through the sense of touch.

Dr. Tan was an Associate Editor for IEEE TRANSACTIONS ON HAPTICS, and Editor-in-Chief for the IEEE World Haptics Conference Editorial Board.

Thomas Low received the B.S. degree in mechanical engineering from the University of California, Berkeley, CA, USA and the M.S. degree in mechanical engineering from Stanford University, Stanford, CA, USA.

He is the retired Former Director of the Robotics Laboratory. He joined SRI International in 1984. He has led projects in automation and material handling, autonomous vehicles, advanced man–machine interfaces, medical devices and robotics, including the Extreme Environment Missions deployment of teleoperated robotic systems, drug delivery devices, and blood and plasma processing instruments. He has experience in program management, robotics, software development, mechanical design, medical product development, computer-aided engineering, design for manufacturability, electromechanical systems, sensor development, real-time computer graphics, and dynamic simulation. Until recently, he lead a team of engineers and scientists in developing new robotic systems and technologies for commercial and government clients. He is currently a Senior Technical Advisor with SRI, Menlo Park, CA.

Stephen P. Beaudoin received the B.S. degree in chemical engineering from the Massachusetts Institute of Technology, Cambridge, MA, USA in 1988, the M.S. degree in chemical engineering from the University of Texas at Austin, Austin, TX, USA, in 1990, and the Ph.D. degree in chemical engineering from North Carolina State University, Raleigh, NC, USA, in 1995.

He is a Professor with the School of Chemical Engineering, Purdue University, West Lafayette, IN, USA, where he also serves as the Founding Director of the Purdue Energetics Research Center. He also serves as Academic Director of the Dual M.S. in defense engineering and technology degree program, which is jointly offered by Purdue and Cranfield University (U.K.).

Bryan W. Boudouris received the B.S. degree in chemical engineering from the University of Illinois at Urbana-Champaign, Champaign, IL, USA, in 2004, and the Ph.D. degree in chemical engineering from the University of Minnesota, Minneapolis, MN, USA, in 2009.

He conducted postdoctoral research from 2009 to 2011 with the University of California, Berkeley and Lawrence Berkeley National Laboratory. He is currently a Professor with the Charles D. Davidson School of Chemical Engineering and a Professor (by courtesy) with the Department of Chemistry, Purdue University, West Lafayette, IN, USA, where he is also serving as the Associate Vice President for Research, Strategic Interdisciplinary Research.

William G. Haris received the B.S. degree in mechanical engineering from the Univeristy of Maryland, College Park, MD, USA, in 1993, and the M.S. degree in electrical and computer engineering from the Johns Hopkins University, Baltimore, MD, in 2016.

He is currently a Robotics Engineer with the Naval Surface Warefare Center, Indian Head, MD. He performs research and engineering in robotics technology related to unmanned systems and their associated subsystems. His graduate studies focused on advancing low-cost multidigit myoelectric hand prosthesis, and his research interests include unmanned systems integration and applications in machine learning.

Juan P. Wachs (Senior Member, IEEE) received the B.Ed.Tech. degree in electrical education from ORT Academic College, Hebrew University of Jerusalem, Jerusalem, Israel, in 1995, and the M.Sc and Ph.D. degrees in industrial engineering and management from the Ben-Gurion University of the Negev, Beersheba, Israel, in 2003 and 2008, respectively, .

He is a University Scholar and a Full Professor with the School of Industrial Engineering, Purdue University, West Lafayette, IN, USA, and a Professor of biomedical engineering (by courtesy) and an Adjunct Associate Professor of surgery with Indiana University School of Medicine, Indianapolis, IN. He is also the Director with the Intelligent Systems and Assistive Technologies (ISAT) Lab, Purdue University, and he is affiliated with the Regenstrief Center for Healthcare Engineering.